The Influence of Changes in Vegetation Type on the Surface Energy Budget

Runhua Yang, J. Shukla,
Center for Ocean-Land-Atmosphere Studies 4041 Powder Mill Road, Calverton, MD 20705, USA
and *P.J. Sellers*
NASA / GSFC 923, Greenbelt, MD 20771, USA
Received May 3, 1993, revised October 14, 1993

ABSTRACT

The influence of changes in vegetation type on the surface energy budget was studied using the Simple Biosphere Model (SiB) of Sellers et al. (1986). The modeled energy budget response to the conversion of forest to short vegetation or bare soil (deforestation) was investigated with SiB forced by three time-series of atmospheric boundary conditions collected at three different climatic sites: an Amazonian tropical forest, a U.S. Great Plains grassland, and a central Wales spruce forest. The results show that SiB can simulate realistic surface energy budgets and surface temperatures, and that deforestation may have a significant influence on the local surface energy budget and surface weather. The influence is especially prominent at the Amazonian and U.S. Great Plains sites, and greater in summer than in other seasons.

It was found that atmospheric boundary conditions play a dominant role in determining the degree of changes in the surface fluxes and temperature induced by deforestation; the largest change in latent heat flux appeared at the Amazon site, the largest change in sensible heat flux appeared at the Spruce forest site, and the largest change in surface temperature appeared at the Great Plains site. The Bowen ratios of the SiB sensitivity integrations for each site are comparable with observations. The values of the Bowen ratio and the ratio of latent heat flux to net radiation vary distinctly from site to site, implying that local atmospheric conditions limit the range of changes caused by the vegetation change.

Key words: Biosphere model, Vegetation effect, Sensitivity test, Land-atmosphere interaction

I. INTRODUCTION

In the last decade, parameterizations of land surface processes (LSPs) in atmospheric general circulation models (GCMs) have become more realistic and grown in sophistication. Modeling schemes include more accurate representations of the processes associated with vegetation. Three well-known biosphere models are the Biosphere-Atmosphere-Transfer scheme model (BATS, Dickinson, 1984a; Dickinson, et al., 1986), Simple Biosphere Model (SiB, Sellers et al., 1986), and the Land Ecosystem-Atmosphere Feedback Model (LEAF, Lee et al., 1991). Both BATS and SiB have been implemented in GCMs, and LEAF is used in a mesoscale model. These biosphere models account for both the effects of precipitation interception by vegetation, and the control on the evaporation rate exerted by vegetation canopies and root systems. In addition, some models determine the surface albedo, soil moisture, and surface roughness as mutually consistent functions of the prescribed vegetation parameters. It is believed that with a more realistic biosphere model the simulation of the effects of changes in vegetation type, particularly the effect of deforestation, as well as the simulation of the hydrological budget, are more reliable and compare well with observations.

(Dickinson and Henderson-Sellers, 1988; Dickinson, 1989; Shukla et al., 1990; Henderson-Sellers et al., 1990; Nobre et al., 1991).

In these biosphere models, the change in vegetation type is represented by a change in the set of vegetation parameters which determine the surface albedo, the surface roughness, and the formulations affecting the evaporation rate. The change in albedo will modify the total energy available; the change in surface roughness will influence the momentum transfer and moisture convergence; and the change in evapotranspiration will redistribute the partitioning of incoming radiative energy into fluxes of sensible and latent heat. Changes in the surface fluxes also affect the overlying atmosphere which in turn feedback, positively or negatively, on surface processes, constituting a complete interactive cycle.

Since this study applies SiB at single points, rather than within GCMs, we will review only the results from previous similar applications. The evaluations of SiB performance have been made for several sites by comparing it with observational micrometeorological data (Sellers and Dorman, 1987; Sellers et al., 1989). The comparisons show that, in general, the predicted values of sensible and latent heat fluxes, surface temperature, and other biophysical variables agree with observations. The sensitivity tests of individual parameters show that the partitioning of available energy into ground heat flux, sensible heat flux and latent heat flux is the process most sensitive to changes in the parameters. The evapotranspiration process is sensitive to the physiological properties of the vegetation, such as leaf stomatal resistance parameters, leaf area index, and plant vascular system resistances. Sellers et al. (1989) further improved the SiB performance at a tropical forest site by considering a triangular description of leaf area density within canopy height and utilizing an optimization technique to determine appropriate physiological parameters for the SiB representation of the tropical forest.

A global check of SiB performance in computing surface albedo, roughness length, and minimum stomatal resistance showed that these derived variables compare reasonably well with appropriate measurements obtained from the literature and have the additional merit of being mutually consistent (Dorman and Sellers, 1989).

This study is designed to make a simple analysis of the influence of changes in vegetation type on the surface energy budget while neglecting the complete feedback interactions through the atmosphere. We ask two questions: *Under the same atmospheric boundary conditions does the influence of vegetation on the surface energy budget depend significantly on vegetation type? How much does this influence vary with different climate zones*? The potential application of this study is two-fold. First, it investigates the local effects of vegetation changes while the local incident radiative fluxes and precipitation rates remain, theoretically, the same. Second, it explores the errors which occur when presuming homogeneity of surface land properties within a GCM grid box as opposed to the large nonhomogeneities of vegetation type and soil properties that actually occur.

This paper is organized as follows: In Section II, the concepts of SiB are briefly reviewed. The experimental design and the data description are given in Section III. In Sections IV, V, VI, the effects of changes in vegetation type at the Amazon, central Wales, and Great Plains sites are described. Finally, Section VII discusses the results of this study and lists the conclusions.

II. REVIEW OF THE SIMPLE BIOSPHERE MODEL

Since a comprehensive description of SiB is given in Sellers et al. (1986), we present only a brief review here. In SiB, the world vegetation is divided into two morphological groups: trees or shrubs, which constitute the upper story canopy vegetation, and ground cover, which

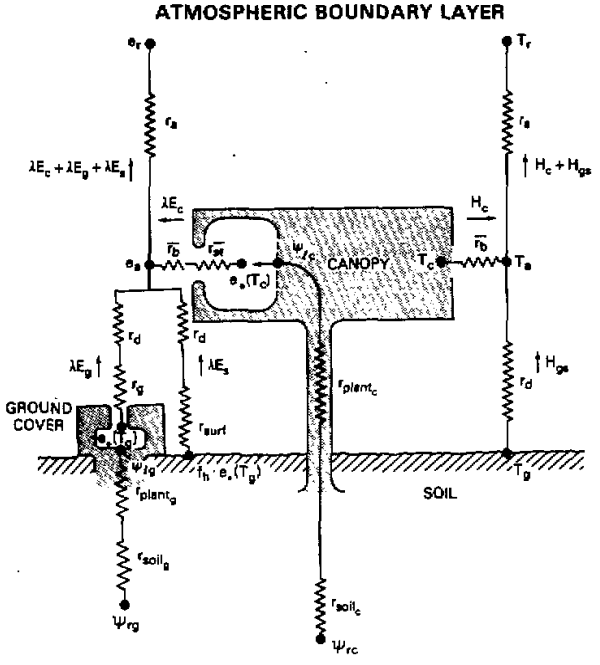

Fig. 1. The framework of the aerodynamic resistance submodel and the surface resistance submodel in SiB. The transfer pathways for latent and sensible heat fluxes are shown on the left-hand and right-hand sides of the Figure.

consists of grasses and other herbaceous plants. SiB vegetation parameters are composed of three groups: morphological, physiological and physical parameters as shown in Sellers et al. (1986, 1989). The soil structure is represented as three layers. The first is a thin, upper soil layer from which direct evapotranspiration can cause a significant withdrawal of water when the soil pores are at or near saturation. The second layer is the root zone of the upper story vegetation and the ground cover. The third layer is the recharge layer where the transfer of water is governed only by gravitational drainage and hydraulic diffusion. The eight prognostic variables in SiB are: three temperature variables (canopy, ground, and deep soil layer), two liquid water storage variables (canopy foliage and ground foliage), and three soil wetness variables (three soil layers).

The atmospheric boundary forcing terms used to drive SiB are: air temperature, vapor pressure, wind speed, precipitation, and the incident radiant flux from the lowest layer of the model atmosphere. When using observations, these forcing terms are provided by measurements taken a few meters above the canopy. The incident radiant flux is partitioned into five components: thermal infrared diffuse flux; visible direct beam and diffuse radiation fluxes; and near infrared direct beam and diffuse radiation fluxes. The morphological and physiological characteristics of the vegetation community within a grid box are used to derive the coefficients which govern the fluxes of radiation, sensible heat, latent heat, and momentum between the surface and the atmosphere. These fluxes are then returned to the overlying

atmosphere and affect the subsequent development of the atmospheric circulation.

SiB consists of three submodels, namely the radiative transfer submodel, the aerodynamic resistance submodel, and the surface resistance submodel. In the radiative transfer submodel, a two-stream approximation is used following Dickinson (1984b) and Sellers (1985). The upwelling diffuse radiation fluxes, surface spectral reflectance, and the radiation absorption are calculated in sequence, and then the net radiation fluxes of the canopy and ground are obtained.

The framework of the aerodynamic resistance and surface resistance submodels is illustrated in Fig. 1 (from Sellers et al., 1986). The sensible heat flux and latent heat flux from the ground to the atmosphere each consists of the two components: the fluxes from the ground to the canopy air space and the fluxes from the canopy vegetation to the canopy air space. The transfer of sensible heat flux is controlled by three aerodynamic resistances including: r_a, the resistance between the canopy air space and the reference height; $\bar{r}_b$, the bulk boundary layer resistance; and r_d, the resistance between the ground and the canopy air space. The transfer of water vapor must also traverse these three resistances but in addition is controlled by three surface resistances: $\bar{r}_c$, the bulk stomatal resistance of upper story vegetation; r_g, the bulk stomatal resistance of ground vegetation; and r_{surf}, the bare soil surface resistance. The three aerodynamic resistances and the three surface resistances are derived by an aerodynamic resistance submodel and a set of surface resistance submodels, respectively (Sellers et al., 1986, 1989).

Table 1. Summaries of the forcing data and vegetation data sets for the experiments

Set	Input forcing data	Vegetation type
1	Observational micrometeorological data at a Amazon site: (2°57′S, 59°57′W)	Type 1: tropical forest
	Data record: Sept 3 1983–Dec. 31 1985	Type 7: ground cover (grass)
	Data description: Shuttleworth et al. (1984)	Type 9: broadleaf shrubs with bare soil
	Moore (1986), Lloyd and Manques (1988)	Type 11: bare soil
2	Observational micrometeorological data at a Norway spruce site, Central Wales, U.K. (52°28′N, 3°42′W)	Type 4: needle-leaf evergreen trees
	Data record: May 31–Dec. 31 1975	Type 7: ground cover (grass)
	Data description:	Type 9: broadleaf shrubs with bare soil
	Sellers and Dorman (1987)	Type 11: bare soil
3	The output of SiB–GCM at the lowest model level over 4 grid points in the Great Plains (32.5–34.4°N, 95.6–92.8°W)	Type 4: needle-leaf evergreen trees Type 7: ground cover (grass) Type 3: broadleaf and needleleaf trees
	Data record: 11 June–11 July 1979	Type 12: broadleaf deciduous trees with winter wheat
	Data description: COLA SiB–GCM output, see text	

III. EXPERIMENT DESIGN

The experiments consisted of three sets of SiB integrations with different vegetation types forced by three time-series of atmospheric boundary conditions. For each set, SiB was inte-

grated repeatedly with each vegetation type forced by the same time-series of atmospheric boundary conditions. Two boundary condition data sets were provided by observations at an Amazon site and a Spruce forest site; the other was taken from the outputs of a version of Center for Ocean-Land-Atmosphere Interactions (COLA) GCM coupled with SiB at the lowest atmospheric model level for four grid points in the Great Plains. Brief descriptions for these three forcing data and vegetation data are listed in Table 1, and the details of the forcing data are described in later sections.

The range of vegetation types used in the study represents the various stages of deforestation: from forest to grassland, and then to desert with shrubs, and to bare soil. Each SiB vegetation type is prescribed by a set of vegetation parameters including soil physical and surface aerodynamic properties. In this study these parameters do not vary with time. Table 2 compares the most important parameters associated with the vegetation types used here. The vegetation cover, green leaf fraction, root length density, and minimum stomatal resistance are specified from a variety of in situ observations reported in the literatures (Sellers and Dorman, 1987). Roughness length (Z_0), the coefficient of the bulk boundary layer resistance $C_1(\bar{r}_b)$, the coefficient of the aerodynamic resistance between the ground and the canopy air space $C_2(r_d)$, are computed using procedures outlined in Sellers et al. (1989).

Table 2. The most important parameters associated with each vegetation type (June) used in the study

vegetation character	TYPE 1	TYPE 4	TYPE 7	TYPE 9	TYPE 11	TYPE 12
vegetation cover (%)	98	75	90	10	1	8
green leaf fraction (%)	91	90	81	57	0	84
root length density (m / m^3)	19737.8	9733.3	9375.0	5500.	1.0	950.
roughness length (m) (Z_0)	2.362	0.88	0.078	0.064	0.011	0.52
$C_1(\bar{r}_b)$	7.21	1.07	20.65	97.34	39034	75.81
$C_2(r_d)$	503.77	1189.30	70.20	27.30	28.04	232.14
min. stomatal resistance (s / m)	45	70	40	---	---	150

The analysis included three procedures. First, we verified three simulations: the integration in set 1 with tropical forest, the integration in set 2 with needle-leaf evergreen trees, and the outputs of the COLA GCM averaged for four grid points in the Great Plains in set 3. These verifications documented the model's ability to reproduce the observed fluxes over the appropriate existing vegetation type and also provided information for the subsequent sensitivity tests. Second, we analyzed the differences between the simulations and the results of sensitivity tests within a set and determined the impact of the vegetation change on surface fluxes and meteorological variables. Finally, we compared the results among the three sets to explore how the influence of vegetation varies with different atmospheric boundary conditions or climate zones.

IV. SiB SENSITIVITY TO VEGETATION CHANGE AT THE AMAZONIAN SITE

1. *Data description*

Routine meteorological measurements were made by two automatic weather stations mounted at a height of 45 m on an aluminum scaffolding tower at 2°57′S, 59°57′W in the Reserve Florestal Ducke, 25 km from Manaus, Amazon Brazil. The forest canopy consists of many species and is typical of an undisturbed natural forest. It extends with no obvious sub-stories to a height of 35 m with occasional emergent trees reaching 40 m. The measurement interval was 5 minutes, and then the hourly values were averaged. Data records covered the period from September 3, 1983 to September 30, 1985. The data collection and analysis procedures were described by Shuttleworth et al. (1984), Moore (1986), Lloyd and Marques (1988).

The monthly means of the meteorological variables measured at 45 m (the measurement height will be referred to as the reference height) were computed for 25 months. Figure 2 illustrates the monthly mean precipitation, also shown as points with bars are the means and standard deviations of the monthly mean precipitation, also shown as points with bars are the means and standard deviations of the monthly precipitation measured at a nearby climatological station for the years 1965 to 1981 (from Shuttleworth, 1988). The climatological average rainfall exhibits a marked seasonal dependence with a maximum in March and a minimum in August. There is also a clear division between the dry season (from June to November) and the wet season (from December to May). The rainfall observed during the period from September 3, 1983 to September 30, 1985 is clearly representative of the climatological annual cycle except in December 1983 when the precipitation was anomalously heavy. The monthly mean net radiation (not shown) is relatively low during the wet season and relatively high during the dry season with sharp changes from the warm months to the cool months. The interannual variations are quite large, such as a 25 Wm^{-2} difference between November 1984 and November 1983.

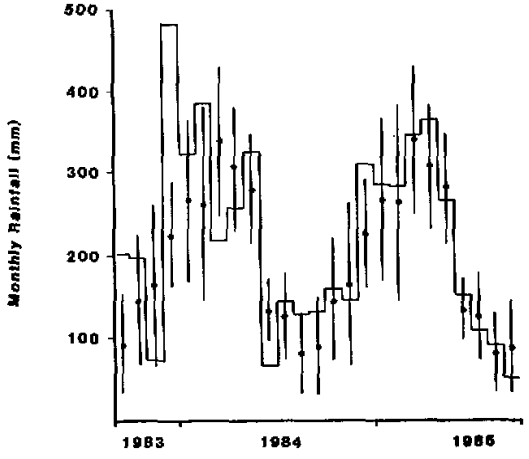

Fig. 2. Monthly precipitation as measured at the Amazon site over the 25 month experimental period. Also shown are the means (points) and standard deviations (bars) of monthly precipitation measured at a nearby climatological station for the years 1965–1981.

The monthly mean temperatures vary little. A minimum temperature of 24°C occurred in February 1984 and a maximum temperature of 27°C in September 1983. As expected, the temperatures are high during the dry season and low during the wet season in agreement with the variation of net radiation and precipitation. The monthly mean vapor pressures are always higher than 26 hPa, and their variations are less than 3 hPa. The standard deviation of hourly temperature is high during the warm season with a maximum of 3.8°C and lower in the cool season with a minimum of 3.0°C. The standard deviations of hourly vapor pressure are generally confined to 1–2 hPa and do not show seasonal change.

The above statistics show that the Amazon site has characteristics of a tropical forest climate: warm and moist with small diurnal and seasonal variations in temperature, vapor pressure, and wind speed. The averaged monthly means and standard deviations of the above variables from June to December are listed in Table 3.

Table 3. The monthly means of surface net radiation (R_n), air temperature (T_m), vapor pressure (e_m), wind speed (U_m), the standard deviations of hourly temperature S.D. (T_m), and vapor pressure S.D. (e_m), computed from measurements (or GCM run) at the reference height above the three sites for the experimental period. Site 1 is in Amazonia, site 2 is in Central Wales, and site 3 is in the Great Plains

VAR	SITE	JUNE	JULY	AUG.	SEPT.	OCT.	NOV.	DEC.
R_n (W/m^{-2})	site 1	119	122	122	136	117	116	99
	site 2	139	127	99	60	33	13	2
	site 3	224						
T_m(°C)	site 1	25.2	25.2	25.6	26.4	25.7	26.3	24.8
	site 2	12.6	15.4	15.8	9.5	5.5	2.1	2.7
	site 3	27.3						
e_m (hPa)	site 1	27.0	26.6	27.0	27.2	28.2	28.0	28.0
	site 2	12.2	14.5	16.2	10.9	8.6	6.8	7.1
	site 3	18.9						
U_m (m / s)	site 1	1.54	1.57	1.62	1.52	1.39	1.50	1.29
	site 2	1.29	0.89	0.90	1.29	1.18	1.23	1.44
	site 3	3.70						
S.D. (T_m)	site 1	3.25	3.45	3.55	3.61	3.41	3.58	3.33
	site 2	8.20	7.20	7.20	6.11	6.50	5.71	4.47
	site 3	4.70						
S.D. (e_m)	site 1	2.16	1.59	1.73	1.62	1.51	1.48	1.58
	site 2	4.40	3.81	4.70	3.00	2.90	2.40	1.80
	site 3	3.20						

2. *Simulation*

A 25-month simulation was performed by using SiB with tropical forest vegetation. During the entire 25 months there are only 19 days with a full 24 hours of observed sensible heat and latent heat fluxes. A comparison of the observed and simulated sensible heat fluxes for the 19 days is shown in Fig. 3. The date is given at the top of each corresponding diurnal cycle, and the values shown on the horizontal axis are cumulative hours over each 10-day period. The solid line denotes the observations and the dashed line with dots denotes simulation. Of the 19 days, 10 days of simulation are close to the observed with errors less than the measurement error which is estimated to be about 10% of the flux. The large errors in the

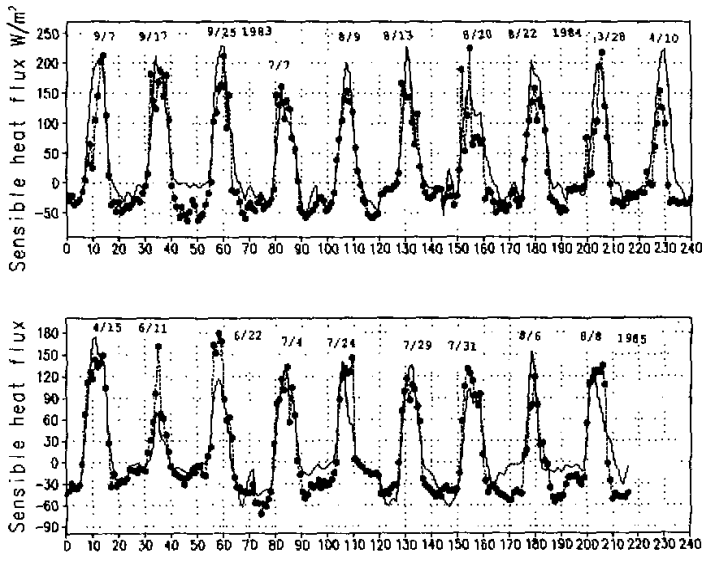

Fig. 3. The hourly simulated and observed values of surface sensible heat flux for 19 days at the Amazon site; the date is shown at the top of the corresponding diurnal cycle. Solid lines are observations, and dashed lines with dots are simulations.

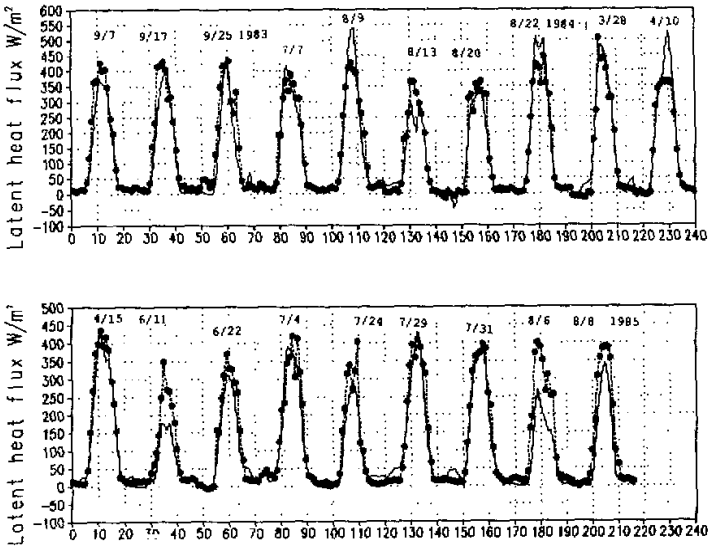

Fig. 4. Same as Figure 3 but for latent heat flux.

simulation occur at the local noontime with maximum errors of about 60 W m^{-2}. The simulation of latent heat flux, with 12 days of good simulation, is generally better than that for sensible heat flux (Fig. 4). The errors in simulated latent heat and sensible heat fluxes on April 10 and June 11, 1985 are large and are of the same sign, indicating an inconsistency in the forcing data or in the flux measurements.

3. *Sensitivity tests*

Three integrations were performed with a grassland (type 7), desert with shrubs (type 9), and bare soil (type 11), respectively forced by the same time-series of atmospheric boundary conditions at the Amazon site. The initial soil wetness was prescribed as 0.63 for all types. For type 1, the downward long wave radiation was calculated as the residual of a surface energy balance equation. For the other vegetation types, the downward longwave radiation was assumed to be the same as type 1 and the net radiation was calculated from the surface energy balance equation. Figure 5 shows the simulated monthly averaged hourly albedo values during the local time period, 7:00 am to 6:00 pm, for the four vegetation types: type 1 had the lowest value of 0.14 to 0.15, and type 11 had the maximum value of 0.32. The variation of the albedo within the day is generally smaller than 0.03. Figures 6–9 show the monthly mean diurnal cycles of four model output quantities in September (left panel) and December (right panel) respectively. September is within the dry and warm season with high net radiation, and December is within the wet and cool season with low net radiation.

The net radiation differences (Fig. 6) respond directly to the albedo differences, type 1 with a maximum value and type 11 with a minimum value. The differences between the vegetation types develop during the day time and reach their maxima at noontime. In September (left panel) the net radiation with vegetation type 7 is smaller than that with vegetation type 1 by 50 W m^{-2}. The largest difference is 160 W m^{-2} between type 1 and type 11. In December the daily maximum is reduced from about 500 W m^{-2} in September to 350 W m^{-2} as the sun moves towards the Tropic of Cancer which has the effect of reducing the differences among the vegetation types. The maximum difference between types 1 and 7 is about 30 W m^{-2}, and between types 1 and 11 is approximately about 100 W m^{-2}. It can be seen that the maximum difference of the net radiation between types 1 and 11 in September is as large as the seasonal changes in net radiation from September to December.

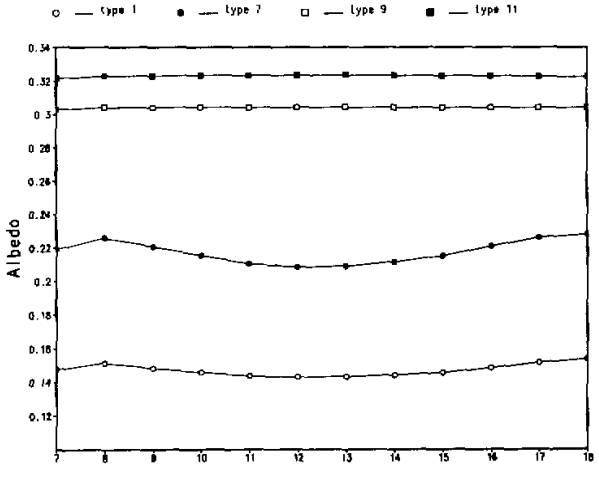

Fig. 5. The simulated mean hourly albedo values during the local time period, 7:00 am to 6:00 pm, for four vegetation types at the Amazon site.

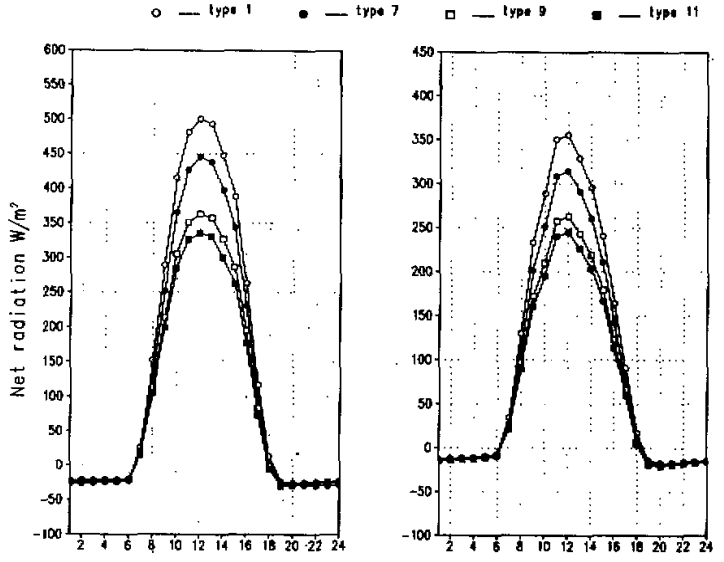

Fig. 6. The diurnal cycles of net radiation in September (left panel) and in December (right panel), averaged for three September months and two December months for the SiB integration starting from September 1983 to September 1985 for four different vegetation types at the Amazon site.

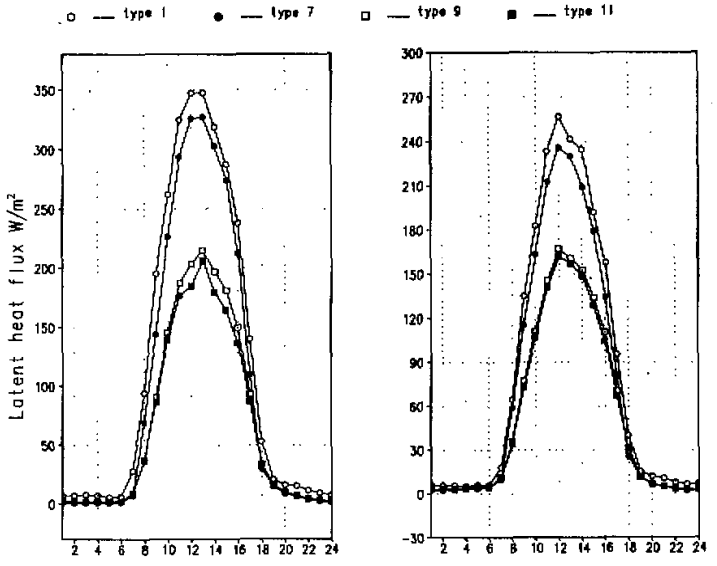

Fig. 7. The diurnal cycles of latent heat flux in September (left panel) and in December (right panel), averaged for three September months and two December months for the SiB integration starting from September 1983 to September 1985 for four different vegetation types at the Amazon site.

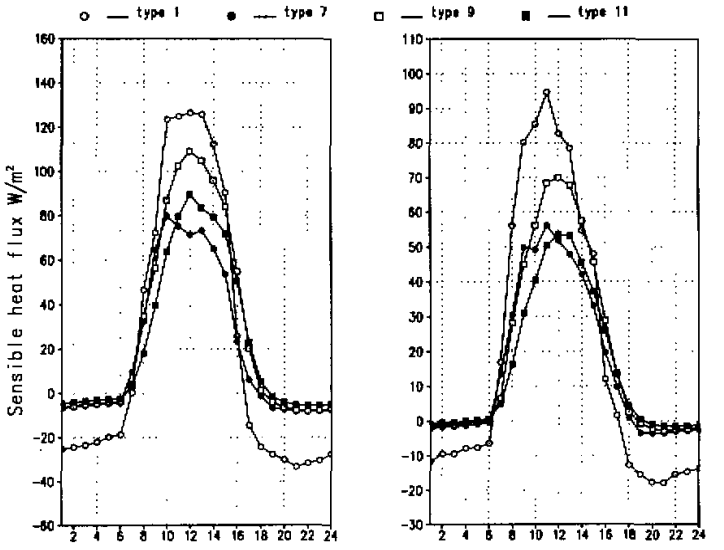

Fig. 8. The diurnal cycles of sensible heat flux in September (left panel) and in December (right panel), averaged for three September months and two December months for the SiB integration starting from September 1983 to September 1985 for four different vegetation types at the Amazon site.

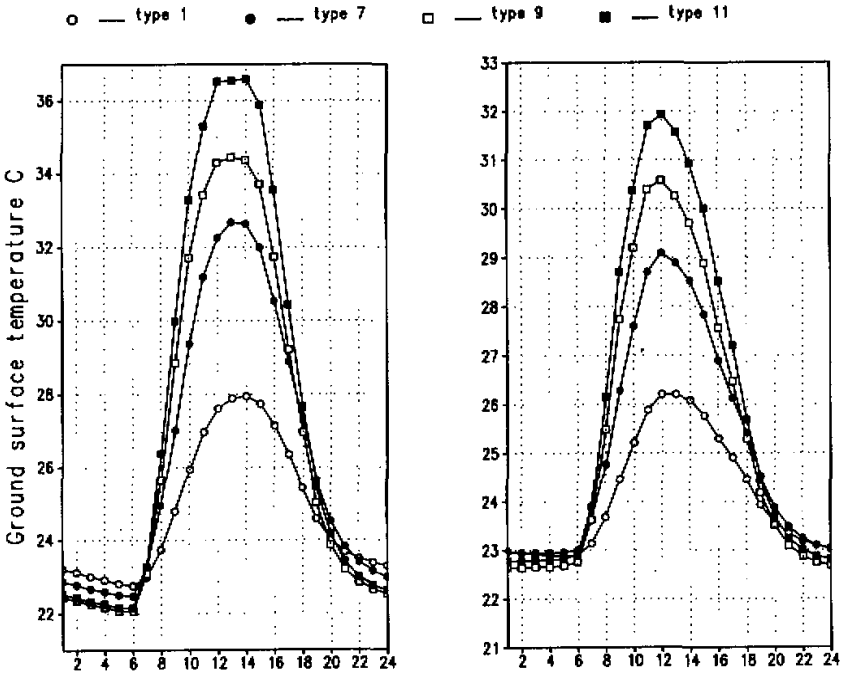

Fig. 9. The diurnal cycles of ground surface temperature in °C in September (left panel) and in December (right panel), averaged for three September months and two December months for the SiB integration starting from September 1983 to September 1985 for four different vegetation types at the Amazon site.

The differences in latent heat flux (Fig.7) are remarkable between vegetation types 1 and 9 or 11. The latent heat flux of vegetation type 1 is consistently larger than those of the other three types, because vegetation type 1 has the densest vegetation cover (see Table 2). During September (left panel), the maximum latent heat flux of both type 9 and type 11 is about 200 W m^{-2}, much lower than the others, due to the reduced vegetation cover and net radiation. The maximum difference in latent heat flux between type 1 and type 11 is about 130 W m^{-2}. During December (right panel), the latent heat flux of each vegetation type is reduced. A maximum difference of 90 W m^{-2} occurs between types 1 and 9. The difference is sensible heat flux (Fig. 8) between vegetation types varies between day and night. During the daytime, the sensible heat fluxes of vegetation type 1 are consistently higher than those of the other types. In contrast, at night the sensible heat flux of vegetation type 1 becomes negative, and that of other types are close to zero. These large nighttime negative sensible heat fluxes are due to the high roughness length of the tropical forest. In September (left panel), a maximum difference of 60 W m^{-2} in sensible heat flux occurs between vegetation types 1 and 7. In December (right panel), the maximum difference occurs between types 1 and 11 with a reduced magnitude of 40 W m^{-2}.

Figure 9 shows that the replacement of vegetation type 1 by the other three types leads to an increase in calculated ground surface temperature. During September (left panel) the maximum afternoon difference is 5°C between types 1 and 7, 6.5°C between types 1 and 9, and about 9°C between types 1 and 11. During December (right) these temperatures are lower, and the differences among these types are relatively small compared to those in September. The maximum differences are about 3°C between types 1 and 7, 4°C between types 1 and 9, and 6°C between types 1 and 11.

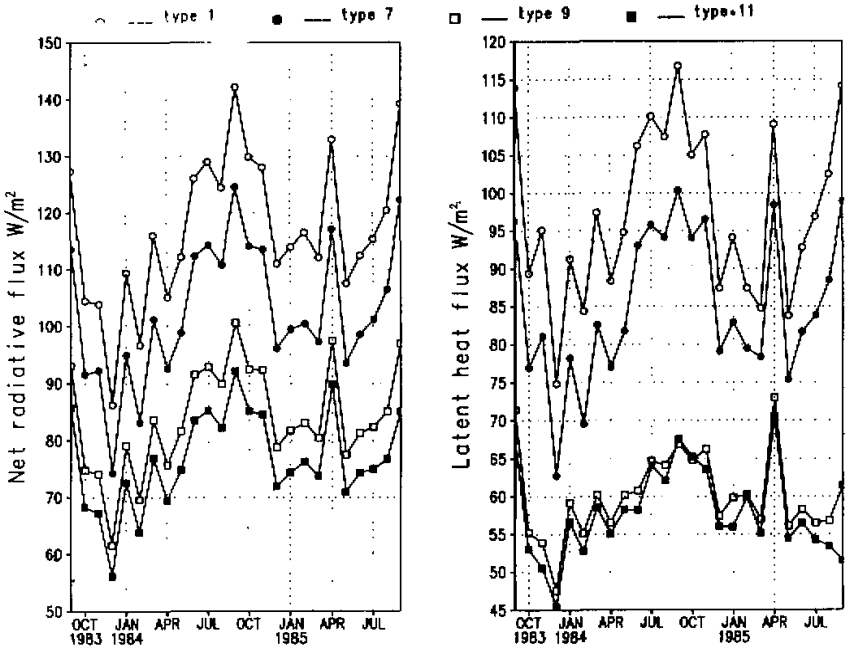

Fig. 10. Monthly means of net radiative flux (left panel) and latent heat flux (right panel), simulated by SiB for four vegetation types for the period September 1983 to September 1985.

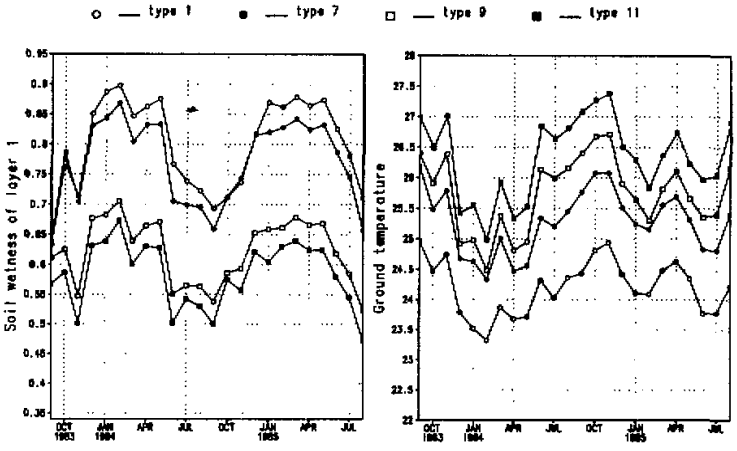

Fig. 11. Monthly means of simulated soil wetness at layer 1 (left panel) and surface ground temperature in °C, simulated by SiB for four vegetation types for the period September 1983 to September 1985.

The month by month variations of several variables for the four vegetation types over the whole 25-month integrations are plotted in Figs. 10 and 11. The differences in net radiation and latent heat flux between these four types (Fig. 10) are consistent during the whole period and vary with the seasons; larger in warm months and smaller in cool months. For example, the difference in net radiation (left panel) between types 1 and 11 reaches at a maximum of 48 W m^{-2} in September 1984 and a minimum of 24 W m^{-2} in December 1984. The difference in latent heat flux (right panel) between vegetation types 1 and 9 or 11 reaches a maximum of 45 W m^{-2} in September 1984 and a minimum of 27 W m^{-2} in February 1985.

Relatively high during the wet and cool months and low in the dry and warm months, the variation in soil wetness of the first soil layer for each vegetation type (left panel of Fig. 11) has a clear seasonal pattern and follows precipitation. The minimum soil wetness appeared in September 1984 due to extensive evaporation during the pervious months which depleted the soil moisture. The differences between types 1 and 7 are small, as are the differences between types 9 and 11. The low water-holding capacity of vegetation types 9 and 11 causes soil wetness to remain relatively low. Similar patterns exist in soil layers 2 and 3. The monthly mean runoff (not shown) shows that types 9 and 11 have relatively high soil moisture values among the four vegetation types.

The difference in ground surface temperature among these vegetation types (right panel of Fig. 11) is large during the period of June to November 1984 (warm and dry months) and small in the period of December 1983 to May 1984 (cool and wet months). The differences varied from 0.7°C to 1.4°C between type 1 and type 7, and from 1.6°C to 2.6°C between type 1 and type 11. The highest surface temperature corresponds to a desert condition. An interesting feature is that replacement of type 1 by any of these three types generates large intraseasonal and interannual variations of ground surface temperature; for example, the maximum intraseasonal variation with vegetation type 11 is about 2.4°C which is about 0.8°C larger than that with type 1.

V. SiB SENSITIVITY TO VEGETATION CHANGE AT A SPRUCE FOREST SITE

1. *Data description*

The data used consist of hourly micrometeorological measurements taken in a clearing a short distance away from a small Norway spruce forest in central Wales, U.K. (52°28′N, 3°42′W). The values were adjusted by comparison with occasional sets of observations recorded with an automatic weather station above the canopy. It was assumed that the adjusted values were representative of conditions at a height of 12 m, roughly 2 m above the canopy (Sellers and Dorman, 1987). The data was collected from May 31 to December 31, 1975 with 30 days of missing data dispersed over the 7 months.

The monthly mean precipitation during the record period is calculated. At this site precipitation mainly occurred from September to December. Before September the monthly mean precipitation was less than 90 mm / month. The maximum amount of 250mm / month occurred in September and the minimum amount of 45 mm occurred in June (the values for July and December were excluded due to large missing data). The monthly mean net radiation had a maximum value of 140 W m^{-2} in June and then gradually decreased. The minimum value is close to zero in December due to low insolation. The temperature has a maximum value of 15.5°C in August and a minimum of 2°–3°C in November and December giving a seasonal variation of around 14°C. The variation of vapor pressure follows that of temperature with a maximum of 16 hPa in August and a minimum of 7 hPa in November and December. The wind speed varied from 0.8 m s^{-1} to 1.4 m s^{-1}. The standard deviations of hourly temperature and vapor pressure are large during warm months and small during cool months. All these quantities change gradually with the seasons.

These monthly mean values are also listed in Table 3. This site is obviously very different from the Amazon site. It represents a middle–high latitude climate: with warm weather in later summer, rainy in early fall, relatively low temperatures and vapor pressures, and relatively large diurnal variations in temperature and evaporation. The seasonal weather transition is gradual.

2. *Simulation*

Figure 12a shows a comparison of cumulative evaporation between the simulated and the observed data during a 40 day period at the Spruce forest site. The observational data during the period of day 19 to day 33 is read from Fig. 1 of Sellers and Dorman (1987). The simulated value is lower than that observed by about 0.6 mm / day. Figure 12b shows the cumulative runoff and evaporation of the model output as well as the cumulatively observed rainfall for 190 days. The sum of runoff and evaporation is about 10 cm less than the rainfall, partly due to the fact that there were no calculations made for the 30 missing data days. If the model runoff is reliable, then the underestimation of evaporation of the model during this period is approximately 0.6 mm / day.

3. *Sensitivity test*

Three integrations were performed with vegetation types 7, 9, and 11 with the same micrometeorological observation data as in the simulation. As with the Amazon site, the downward longwave radiation of type 4 was calculated as a residual from the surface energy balance equation in the simulation and then as input for these three integrations. The integration starts from May 30 to December 31, 1975 excluding the 30 days of missing data. The initial soil wetness was prescribed as 0.63 as before.

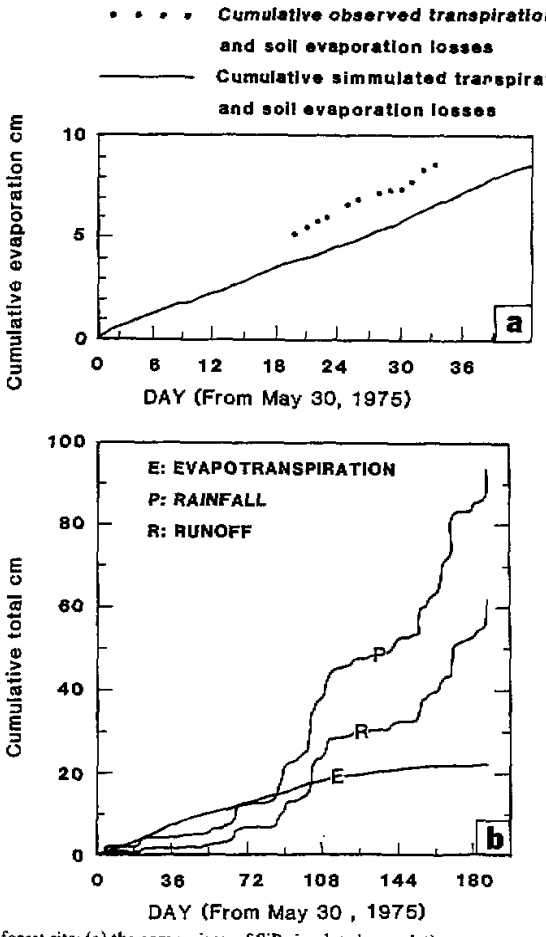

Fig. 12. Spruce forest site: (a) the comparison of SiB simulated cumulative evapotranspiration with observations for a 40-day period starting from May 30, 1975 (b) the comparisons among the simulated cumulative evapotranspiration losses (E) and runoff (R) and the observational cumulative precipitation (P) for the spruce site over a 6 month period starting from May 30, 1975.

The results of the sensitivity test for June are described. This month was chosen because it had large net radiation values which lead to enhanced model sensitivity. The left panel of Fig. 13 shows that the replacement of vegetation type 4 by the three other vegetation types increases mean hourly albedo from 0.11 to 0.22 (type 7), to 0.30 (type 9) and to 0.32 (type 11), respectively. The maximum difference in net radiation (right panel) is 66 W m^{-2} between vegetation types 4 and 7, 116 W m^{-2} between types 4 and 9; and about 140 W m^{-2} between types 4 and 11. Figure 14 shows the surface latent and sensible heat fluxes. The latent heat flux (left panel) of vegetation type 4 is generally higher than those of the other vegetation types. The differences between types 9 and 11 are small. A maximum difference of 75 W m^{-2} exists between types 4 and 9 or 11. The sensible heat flux (right panel) of vegetation type 4 is much

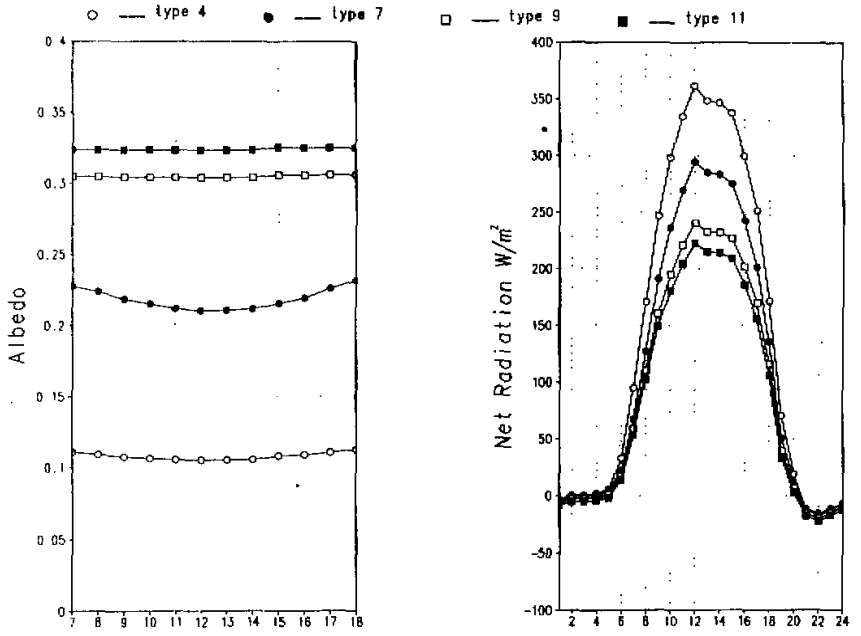

Fig. 13. Spruce forest site: mean hourly albedo values during the local time period, 7:00 am to 6:00 pm (left panel), diurnal cycles of net radiation in June (right panel), as simulated by SiB for four vegetation types.

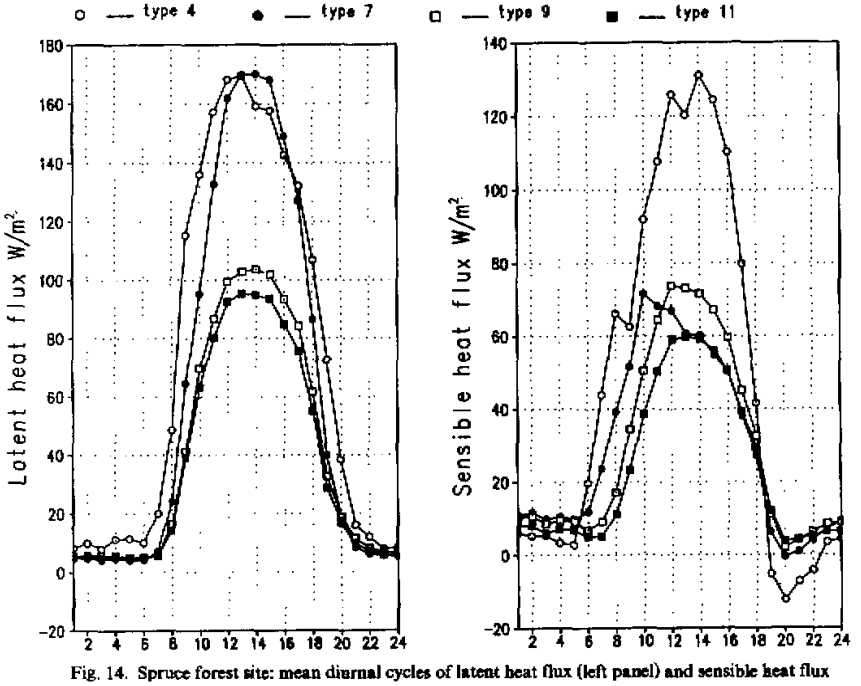

Fig. 14. Spruce forest site: mean diurnal cycles of latent heat flux (left panel) and sensible heat flux (right panel) in June, as simulated by SiB for four vegetation types.

higher than those of the other three types, and vegetation type 11 has the smallest value. The maximum difference is more than 70 W m^{-2} between types 4 and 11, whereas the other three types have small differences. The ground surface temperature differences (not shown) are smaller than that in the Amazon site. The largest daytime difference is about 3.5°C between types 4 and 11. The replacement of vegetation type 4 by the other three vegetation types generally made the ground surface temperatures increase in the daytime and decrease slightly at night.

The month by month variations of net radiation and latent heat flux for the four vegetation types are illustrated in Fig. 15. The left panel of Fig. 15 shows that the monthly mean net radiation gradually decreased as the sun moved southward and became less than one half of the June amount by September. Compared with this figure, the differences in hourly net radiation among different vegetation types are even larger than the seasonal changes. In conjunction with the decrease in net radiation, the differences among these four vegetation types also decreased. In June, the difference between types 4 and 11 is 60 W m^{-2}, but the difference is only 30 W m^{-2} in September. The differences in the calculated latent heat fluxes (right panel of Fig. 15) between types 4 and 7, between types 4 and 9 or type 11, were large during the summer but diminished remarkably after September.

The sensible heat flux (not shown) of vegetation type 4 was much larger than those of the other three types before September, but thereafter dramatically decreased to values close to

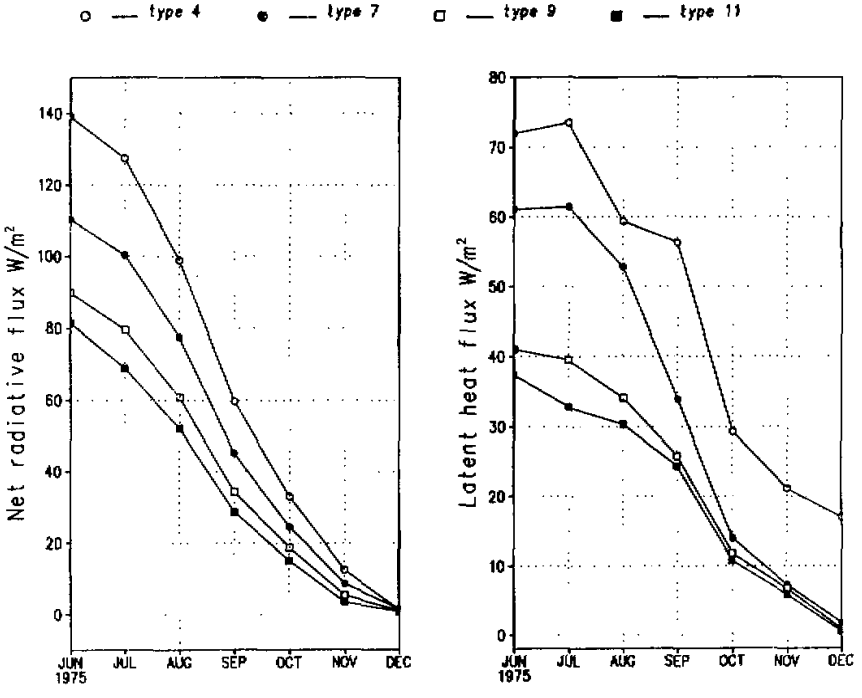

Fig. 15. Spruce forest site: monthly means of net radiative fluxes (left panel) and latent heat flux (right panel), as simulated by SiB for four vegetation types for the period of May to December 1975.

those of other three types. The soil wetness of layer 1 for each vegetation type decreased starting in June and reached a minimum in July due to large evaporation losses that month. Afterwards, soil wetness gradually increased again. The soil wetnesses of types 4 and 7 are as high as 0.84, but the values of types 9 and 11 are small due to their low water-holding ability. The differences among these types are small before September and became large during the winter. The differences in monthly mean ground surface temperature among these four types (not shown) are no more than 1°C with the largest difference in September between vegetation type 4 and the others.

VI. MODEL SENSITIVITY TO VEGETATION CHANGES AT THE GREAT PLAINS SITE

1. *Data description*

A one month-long time-series of meteorological boundary conditions was generated by averaging the relevant variables of SiB-GCM outputs for the lowest atmospheric model layer for four adjacent grid points in the Great Plains. The hourly mean data were averaged from the 12 minute output, The time period studied was from June 11 to July 10, 1979. The 4-point averaged 30-day mean temperature at the lowest model level (45 m, approximately) was 27°C, the averaged vapor pressure was 18.9 hPa, the mean net radiation was 224 W m^{-2}, and the precipitation was 41.17 mm / month. The wind speed was much higher than at the other two sites since the model consistently produced too high a surface wind speed compared with observations. The standard deviations of hourly temperature and vapor pressure were 4.7°C and 3.2 hPa respectively, values that are between the values of the other two sites (see Table 3). It is clear that the weather of this site is different from the Amazon and Spruce sites: it is warmer than the other two sites, wetter than the Spruce site but drier than the Amazon site, and monthly variances of temperature and vapor pressure reside between the two.

2. *Simulation and sensitivity test*

Figure 16 shows comparisons between the observed and GCM simulated 30-day averaged diurnal cycles of surface air temperature (part a) and relative humidity (part b) averaged over the four grid points. Overall the 30-day mean diurnal cycles of predicted temperature and relative humidity are close to observations. The maximum error in hourly temperature simulation is about 2°C, but the 30-day mean simulated temperature error was less than 1°C. The mean relative humidity simulation was good during the daytime but had more than a 10% error during the night.

Assuming that the four-point averaged downward longwave radiation of the GCM output does not change with the different vegetation types, the integration was performed from June 11 to July 11, 1979 for each vegetation type with the same initial soil wetness.

Figure 17 shows calculated net radiation (left panel) and latent heat fluxes (right) for the four vegetation types. Generally the difference in net radiation follows the albedo differences: types 4 and 3 have relatively higher net radiation values due to their small albedos, and the other two types have relatively low values due to their large albedo values. The maximum net radiation for type 7 is about 60 W m^{-2} less than that for type 4, and a maximum difference of 125 W m^{-2} occurs between types 4 and 12. A maximum difference of 180 W m^{-2} in latent heat flux occurs at noon between types 7 and 12, when vegetation type 7 reached a maximum latent heat flux of 400 W m^{-2}. There is little difference between types 4 and 3. Figure 18 shows that the sensible heat fluxes (left panel) of types 7 and 12 are less than that of type 4 by about

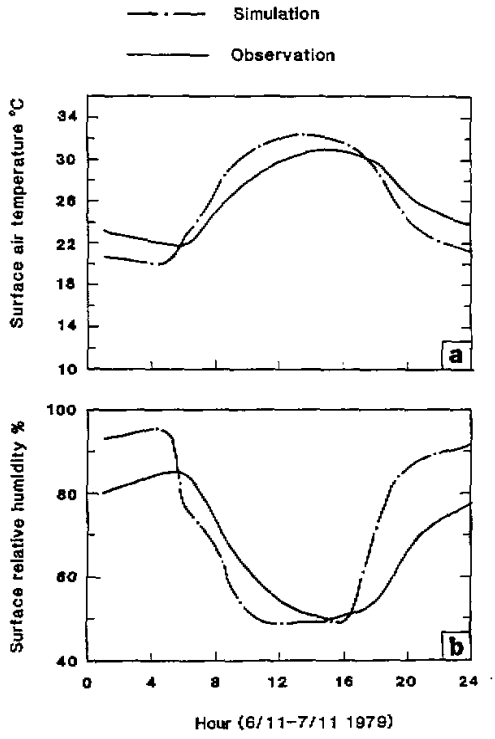

Fig. 16. Comparison of the simulated and observed monthly mean diurnal cycles of (a) surface air temperature and (b) surface relative humidity at four grid points in the Great Plains of the United States, over the period of June 11 to July 11 1979; observation (solid line), and SiB simulation (broken line).

200 W m^{-2} and 170 W m^{-2} respectively. The surface fluxes of types 3 and 4 are close. At night, types 4 and 3 have larger negative sensible heat fluxes than the other two types, because of their large surface roughnesses, which may also generate strong daytime upward sensible heat fluxes and cooler surface temperatures at night. The differences between the ground surface temperature (right panel) are somewhat surprising: the maximum differences is 12°C between vegetation types 12 and 3, while the maximum temperature of type 12 even reaches 45°C. The surface temperatures for type 7 are consistently higher than those of vegetation types 3 and 4, with the maximum difference of about 3°C between types 7 and 3, and about 1.5°C between 7 and 4. The vegetation cover fraction for type 12 during this month was very small, and so its ground surface temperature is expected to be the highest among these vegetation types. Maximum ground surface temperatures as high as 45°C have been observed in arid areas.

The soil wetnesses of types 4 and 3 (not shown) were very similar and close to the initial value of 0.77. The mean soil wetness of type 7 was the smallest among the four vegetation types. It decreased from the initial value 0.77 to 0.5 due to its high evaporation rates which depleted the soil moisture.

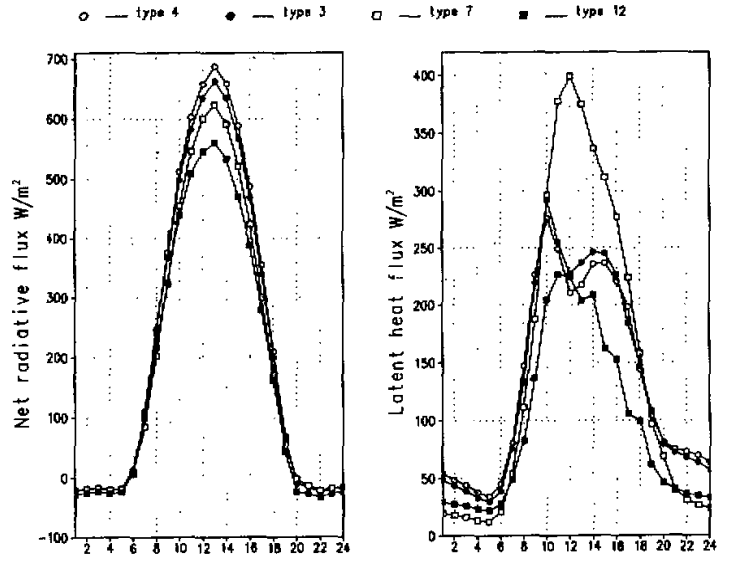

Fig. 17. The Great Plains site: mean diurnal cycles of net radiative flux (left panel), and latent heat flux (right panel), as simulated by SiB for the period of June 11 to July 11 1979 for the four vegetation types.

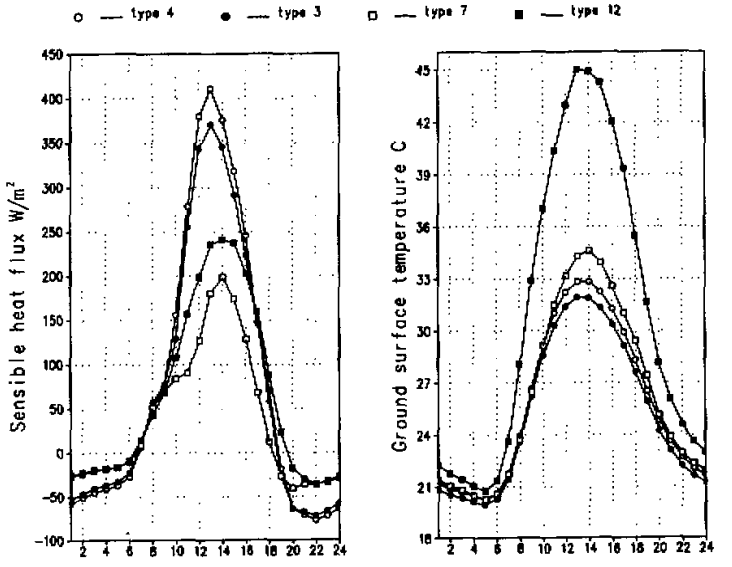

Fig. 18. The Great Plains site: mean diurnal cycles of sensible heat flux (left panel) and ground surface temperature (right panel), as simulated by SiB for the period of June 11 to July 11 1979 for the for vegetation types.

VII. SUMMARY AND CONCLUSIONS

The monthly means of surface net radiation, surface latent heat and sensible heat fluxes, and surface temperatures simulated by SiB with the different vegetation types at the three sites are listed in Table 4. Also shown are the Bowen ratios and the ratios of latent heat flux to net radiation. This table shows that over three different climatic zones there are consistent changes associated with deforestation: decreasing net radiation due to the increase in albedo, decreasing latent heat flux (except with type 7 at the Great Plains site), and increasing ground temperature (little difference at the Spruce forest site). The friction velocity and soil wetness (not shown) are also decreased. At the Amazon and Spruce sites, runoff (not shown) consistently increased as soil water-holding capability was reduced.

The differences in the calculated surface energy partition among forest and ground cover (type 7) and desert (types 9 and 11) are large at all three sites. The differences in surface temperatures are large at both the Great Plains and Amazon sites but small at the Spruce site due to the much lower insolation. The changes in surface temperature, surface net radiation, and surface latent heat flux caused by deforestation, particularly in the mean diurnal cycle, are more prominent at the Amazon and the Great Plains sites (tropical and subtropical climate zones) than in the Spruce forest site (high-middle latitude zone), mainly because of the high net radiation fluxes associated with the former.

It is important to point out that the differences between the monthly means of surface energy flux components associated with changes in vegetation type are smooth compared to the differences in the mean diurnal cycles, especially in the daytime.

There is an interesting feature shown in Table 4: the largest change in latent heat flux appeared at the Amazon site, the largest change in sensible heat flux appeared at the Spruce forest site, and the largest change in surface temperature appeared at the Great Plains site. This suggests that atmospheric boundary conditions largely determine the degree of changes in surface fluxes and temperature caused by deforestation. Furthermore, the values of the Bowen ratio at one site are generally different from those of the other two sites (except at the Great Plains site with type 7, which had enormous latent heat fluxes). The Bowen ratios are small at the Amazon site and relatively large at the Spruce forest site. At the Great Plains site, the values are generally between those of the other two sites. Similarly, the ratios of latent heat flux to net radiation at the three sites are also distinctive. At the Amazon site, evaporation made up a large percentage of the net radiation, about 70–84 percent. At the Spruce forest site, although the surface temperature was low, evaporation still consumed about 45–50 percent of the net radiation. At the Great Plains site, evaporation consumed about 50–60 percent of the net radiation with all types except type 7. These features imply that the local atmospheric conditions limit the range of changes caused by the change in vegetation type. In other words, these two ratios can be used to measure the degree of influence of local vegetation changes at a given site. Finally, the fact that the Bowen ratios in each site are comparable with observations (Shuttleworth et al., 1984; Ji and Hu, 1989) shows that SiB can generate appropriate surface micrometeorological conditions when forced with different atmospheric boundary forcing.

Due to the exclusion of the feedbacks of vegetation type on atmospheric conditions in this study, results here could not depict a full picture of the interactions between the vegetated land and the atmosphere; the most important phenomenon, the change in precipitation, could not be addressed. In addition the prescribed high initial soil wetness made the changes in surface sensible heat flux and ground temperature small. Nevertheless, the main results here are

qualitatively in conformity with those revealed by some 3-D GCM deforestation tests. For example, the Amazonian deforestation sensitivity tests, which were performed by Shukla et al. (1990), Nobre et al. (1991), Dirmeyer and Shukla (1991) and Dickinson (1989), show some common results: an increase in ground surface temperature and runoff, a decrease in soil wetness, and a lengthening of the dry season.

Table 4. The monthly means of net radiation (R_{net}), latent heat flux (LE) and sensible heat flux (H), and ground surface temperature (T_g) generated by SiB surface model with different vegetation types at three sites. Also listed are the Bowen ratio (H/LE) and the ratio of latent heat flux to net radiative flux (LE/R_{net})

SITE	TYPE	R_{net}	LE	H	T_g	H/LE	LE/R_{net}
Amazon	1	136.3	114.9	20.6	24.8	.179	.84
Sept.	7	120.1	98.5	19.7	26.3	0.2	.82
	9	96.9	66.6	28.5	26.7	.43	.69
	11	87.6	62.2	23.3	27.5	.37	.71
Spruce forest	4	139.1	72.0	47.0	13.5	.653	.518
	7	110.4	61.1	29.3	13.4	.480	.553
June 1975	9	89.9	41.0	28.9	13.9	.704	.456
	11	81.4	37.6	23.4	14.6	.626	.460
	4	224.7	132.1	78.5	25.7	.594	.588
The Great Plains	3	216.7	132.0	71.5	25.2	.541	.609
6/11-7/11 1979	7	197.1	145.5	36.7	26.2	.252	.740
	12	179.7	94.2	63.1	30.9	.669	.524

This work was supported by the NASA Grant NAGW-1269, NAGW-557 and NSF Grant ATM-871356702. We would like to thank Mr. J. Dorman for his assistance in this work. We would also like to thank Mr. Michael Fennessy, Drs. Anandu Vernekar, Yongkong Xue and Karen L. Prestegaard for their many important suggestions. Finally, we express our thankfulness to Miss Tammy Yeargin for editing the manuscript.

REFERENCES

Dickinson, R.E., (1984a), Modeling evapotranspiration for three-dimensional global climate models, Climate processes and climate sensitivity, *Geophysical Monograph 29*, Maurice Ewing Volume 5:58-72.

Dickinson, R.E. (1984b), Land surface processes and climate surface albedos and energy balance, *Advances in Geophysics*, **25:** Academic Press, 305-353.

Dickinson, R.E., A. Henderson-Sellers, P. Kennedy and M.F. Wilson (1986), Biosphere-Atmosphere Transfer Scheme (BATS) for the NCAR community Climate Model, NCAR Tech. Note, NCAR/TN-275+STR, Boulder, CO, 69pp.

Dickinson, R.E. (1989), Modeling the effects of Amazonian deforestation on regional surface climate: A review, *Agricultural and Forest Meteorology*, **47:** 339-347.

Dickinson, R. E. and A. Henderson-Sellers (1988), Modelling tropic deforestation: a study of GCM land-surface parameterizations. *Q.J.R. Meteorol. Soc.*, **114:** 439-462.

Dirmeyer, P., and J. Shukla, (1991), The impact on climate of Amazon deforestation in a CGM with interactive clouds, *Fifth Conference on Climate Variations*, Dec. 14-18, Denver, Colorado, 271-273.

Dorman, J.L. and P.J. Sellers (1989), A global climatology of albedo, roughness length and stomatal resistance for atmospheric general circulation models as represented by the simple biosphere model (SiB), *J. of Appl. Meter.*, **28:** 833-855.

Henerson-Sellers, A., A. J. Pitman,a nd R.E. Dickinson (1990), Sensitivity of the surface hydrology to the complexity of the land-surface parameterization scheme employed, *Atmosfera*, **3:** 183-201.

Ji, J. and Y. Hu (1989), Sensitivity testings of the land surface process model, *Chinese Journal of Atmospheric Sciences*, **13:** No. 3.

Lee, T.J., R.A. Pielke, T.G.F,. Kittle, and J.F., Weaver (1991), Atmospheric modeling and its spatial representation of land surface characteristics, Proceeding of first international conference workshop on integrating geographic information systems and environment modeling, Sept. 15–19, 1991, Boulder, U.S.A.

Lloyd, C.R. and A. de O. Marques (1988), Spatial variability in rainfall interception measurements in Amazonian rain forest, *Agric. For. Met.*, **42:** 63–73.

Moore, C.J. (1986), Frequency response corrections for eddy correlation systems, *Bound. Layer Met.*, **37:** 17–35.

Nobre, C.A., P.J. Sellers, and J. Shukla (1991), Amazonian deforestation and regional climate change, *J. of Climate*, **4:** 957–988.

Sellers, P.J., Y. Mintz, Y.C. Sud and A. Dalcher (1986), A simple biosphere model (SiB) for use within general circulation models, *J. Atmos. Sci.*, **43:** 505–530.

Sellers, P.J. (1985), Canopy reflectance, photosynthesis and transpiration, *Int. J. Remote Sensing*, **6:** 1335–1372.

Sellers, P.J., and J.L. Dorman (1987), Testing the simple biosphere model (SiB) using point micrometeorological and biophysical data, *J. Climate Appl. Meteor.*, **26:** 622–651.

Sellers, P.J., W.J. Shuttleworth, J.L. Dorman, A. Dalcher and J.M. Roberts (1989), Calibrating the simple biosphere model for Amazonian tropical forest using field and remote sensing data, Part I: Average calibration with field data, *J. Appl. Meteor.*, **28:** 727–759.

Shukla, J., C. Nobre and P.J. Sellers (1990), Amazon deforestation and climate change, *Science*, **247:** 1322–1325.

Shuttleworth, W.J., J.H.C. Gash, C.R. Lloyd, D.J. Moore, J. Roberts, A.D.O. Marques Filho, G. Fisch, V. De Paula Silva Filho, M. De Nazare Goes Ribeiro, L.C. Molion, L. D.De Abreusa and J. Carlos, A. Nobre, O.M.R. Cabral, S.R. Patel and J. Carvalho De Moraes (1984), Eddy correlation of energy partition for Amazonian forest, *Quart. J. Roy. Met. Soc.*, **110:** 1143–1162.

Shuttleworth, W.J. (1988), Evaporation from Amazonian rain forest, *Proc. Roy. Soc. London*, **B233:** 321–346.